Journal Pre-proofs

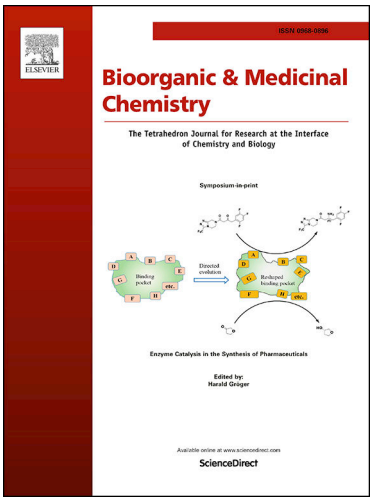

Discovery of Novel Small Molecule Induced Selective Degradation of the Bromodomain and Extra-Terminal (BET) Bromodomain Protein BRD4 and BRD2 with Cellular Potencies

Fei Jiang, Qingyun Wei, Huili Li, Hongmei Li, Yong Cui, Yu Ma, Haifang Chen, Peng Cao, Tao Lu, Yadong Chen

PII: S0968-0896(19)31558-5
DOI: https://doi.org/10.1016/j.bmc.2019.115181
Reference: BMC 115181

To appear in: *Bioorganic & Medicinal Chemistry*

Received Date: 11 September 2019
Revised Date: 18 October 2019
Accepted Date: 24 October 2019

Please cite this article as: F. Jiang, Q. Wei, H. Li, H. Li, Y. Cui, Y. Ma, H. Chen, P. Cao, T. Lu, Y. Chen, Discovery of Novel Small Molecule Induced Selective Degradation of the Bromodomain and Extra-Terminal (BET) Bromodomain Protein BRD4 and BRD2 with Cellular Potencies, *Bioorganic & Medicinal Chemistry* (2019), doi: https://doi.org/10.1016/j.bmc.2019.115181

Bioorganic & Medicinal Chemistry
journal homepage: www.elsevier.com

Discovery of Novel Small Molecule Induced Selective Degradation of the Bromodomain and Extra-Terminal (BET) Bromodomain Protein BRD4 and BRD2 with Cellular Potencies

Fei Jiang[a,b], Qingyun Wei [c,d], Huili Li[a], Hongmei Li[a], Yong Cui[a], Yu Ma[a], Haifang Chen[a], Peng Cao[c,d,*], Tao Lu[a,b,*], Yadong Chen[b,*].

[a] *School of Sciences, China Pharmaceutical University, 639 Longmian Avenue, Nanjing 211198, PR China.*
[b] *State Key Laboratory of Natural Medicines, China Pharmaceutical University, 24 Tongjiaxiang, Nanjing 210009, PR China.*
[c] *Affiliated Hospital of Integrated Traditional Chinese and Western Medicine, Nanjing University of Chinese Medicine, Nanjing 210028, PR China.*
[d] *Laboratory of Cellular and Molecular Biology, Jiangsu Province Academy of Traditional Chinese Medicine, Nanjing 210028, PR China.*

ARTICLE INFO

Article history:
Received
Received in revised form
Accepted
Available online

Keywords:
BRD4 and BRD2
PROTAC degraders
Selectivity
Cancers.

ABSTRACT

The BET proteins BRD2, BRD3, and BRD4 play important roles in transcriptional regulation and can be degraded by proteolysis-targeting chimeras (PROTACs) for BET proteins. However, the lack of intra-BET proteins selectivity limits the scope of current degraders as probes for target validation and could lead to unwanted side effects or toxicity in a therapeutic setting. We describe herein the design, synthesis, and evaluation of PROTAC BET degraders, based on the BET inhibitor with selectivity for the first Bromodomain benzo[*cd*]indole-2-one, alkylamide linker and cereblon ligand thalidomide. Compound **15** potently and rapidly induces reversible, long-lasting, and unexpectedly selective removal of BRD4 and BRD2 over BRD3, which not only effectively inhibits cell growth in human acute leukemia cell lines, but also very effective in inhibiting solid tumors with low cytotoxic effect in the cell profiles of NCI 60 cell lines. Remarkable dependency on linker length was observed for BRD4-degrading and c-Myc-driven antiproliferative activities in acute myeloid leukemia cell line MV4-11. The small-molecular **15** represents a novel, potent, and selective class of BRD4 and BRD2 degraders for the development of therapeutics to treat cancers.

1. Introduction

Bromodomain-containing proteins contain domains that specifically recognize histone acetylation, named "reader". [1] Among them, the bromodomain and extra-terminal domain (BET) family of proteins are the focus of current drug research, which consist of four proteins BRD2, BRD3, BRD4 and BRDT[2]. BET family proteins are nuclear proteins and recruit transcriptional regulatory complexes to acetylated chromatin,[3] which involves in a number of DNA-centered processes including regulation of gene expression. BRD4 recruits a positive transcription elongation factor complex (P-TEFb)[4], which plays a role in the regulation of transcription by RNA polymerase Ⅱ (RNA Pol Ⅱ) in eukaryotes. BET family proteins not only regulate the expression of several important oncogenes (e.g. MYC and BCL2)[5,6], but also cytokines (e.g. IL-17a, TNF-α and IL-6)[7,9]. Therefore, BET proteins have been implicated in a number of human diseases including cancer, inflammation, cardiovascular diseases, human immunodeficiency virus (HIV) Infection and other human diseases[10,12].

Each member of the BET protein contains two bromodomains (the first Bromodomain: BD1 and and the second Bromodomain: BD2) that specifically bind to the acetylated lysine residues of the histone tail to regulate gene transcription. Along with the rapid push of pharmaceutical companies and research institutions, a large number of non-selective first and second bromodomain BET inhibitors were discovered. The **1** ((+)JQ1)[13] with a triazole core structure is represented, and its derivatives include OTX-015[14], I-BET762[15] and other inhibitors are in clinical trials as a new treatment of human cancers. There are reports of BET inhibitors that selective for the second bromodomains, including **2** (BY27)[16], **3** (RVX-208)[17], **4** (GSK340)[18] and **5** (ABBV-744)[19]. Among them, **3** (RVX-208), a selective BET inhibitor of BD2, is in phase Ⅲ clinical trial[17].for the treatment of cardiovascular diseases. Besides, **5** (ABBV-744) developed by Abbvie is currently in phase Ⅰ clinical trials for the treatment of in acute myeloid leukemia (AML) and androgen receptor (AR) positive prostate cancer[19].

The concept of the proteolysis-targeting chimeras (PROTACS) was proposed by Deshaies and Crews in 2001[20]. Great attention has been paid for PROTAC strategy because of its prospects in discovering and developing new types of small molecule therapies. The PROTAC molecule usually consists of three parts: a target protein ligand, an E3 ubiquitinated ligase ligand and a ligation module. Therefore, the molecule not only binds to the target protein but also recruits the E3 ligase complex and degrades the target protein after ubiquitination. In recent years, many laboratories have developed many BET protein degradation

agen ows strategy, including **7** (dBET1)[21], **8** (ARV-771)[22], **9** (QCA570)[23], **10** (BETd-260)[24] and **11** (A1874)[25] as shown in **Figure 1**. In 2015, Winter GE et al. reported the first BET family protein degradation agent, **7** (dBET1), which induced highly selective cereblon-dependent BET protein degradation in vitro and in vivo and delayed leukemia progression in mice. In addition, **9** (QCA570) and **10** (BETd-260), designed and developed by Dr. Shaomeng Wang, contains the cereblon ligand similar to the design of **7** (dBET1). QCA570 induces complete degradation of BET protein prominent growth inhibition in the RS4;11 and MV4;11 xenograft models in mice. In comparison, **8** (ARV-771) was designed by Arvinas based on the von Hippel−Lindau E3 ubiquitin ligase ligand and the BET inhibitor **1** ((+)JQ1). This ligand can suppress both AR signaling and AR levels and leads to tumor regression in a CRPC mouse. **11** (A1874)[25] is firstly reported that the E3 ligase ligand and targeting warhead combine to exert a synergistic anti-proliferative effect.

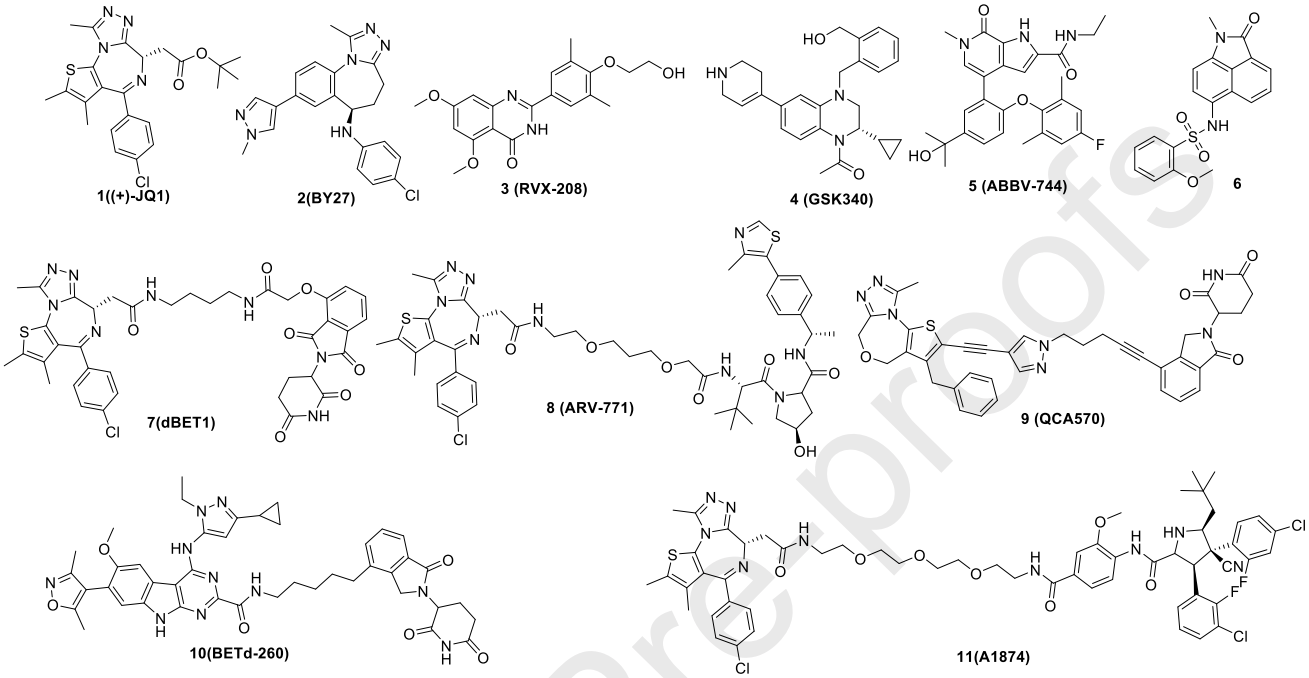

Figure 1. Chemical structures of representative BET inhibitors and five representative previously reported BET degraders.

The BET proteins have achieved great success in treating tumors. However, pan-BET inhibitor with the lack of intra-BET selectivity limits the scope of current drugs as probes for target validation and could lead to unwanted side effects or toxicity in a therapeutic setting. Benzoindole derivatives have been reported to have potential therapeutic cancers[26-27]. In the previous experimental work, our laboratory obtained compound **6** with selectivity for BRD4 BD1. The IC_{50} values of **6** tested using AlphaScreen assay were 49.5±10.3 nM and 2479±170 nM for BRD4 BD1 and BRD4 BD2, respectively, thus about 50-fold selectivity.

Herein, we describe the design, synthesis, and evaluation of novel PROTAC degraders, basing on selective-BD1 BET inhibitor **6**. We identified degrader which is highly potent against leukemia cell line MV4-11 and a variety of solid tumor cells in the NCI cell bank, including, MDA-MB-231, MDA-MB-468, SK-MEL-5 and SNB-75. The BET degrader was able to induce a degraduation of BRD4 protein in a time-dependent and dose-dependent manner. Moreover, representative compound showed depletion selectivity for BRD4 and BRD2 over BRD3 with cellular potencies, low cytotoxicity and induction of cell apoptosis for treating cancers.

2. Results and discussion

To further evaluate the selectivity of **6** to the Bromodomain family, we used the differential scanning fluorimetry (DSF) to test the ΔT_m value of 48 bromodomains at a concentration of 10 μM (**Figure 2B** and **Figure S1** in Supporting Information). The results of compound **6** vs. bromodomains showed that not only the BET family protein was selected to have a ΔT_m value greater than 4.5 °C, but also the binding of BD1 was better than BD2 in the BET family. Furthermore, it exhibits moderate ΔT_m values for BRPF1B and TAF1B in the non-BET family.

Table 1. Binding Affinities of BET Inhibitors

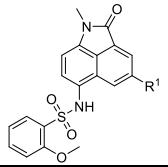

Compound	R^1	Binding affinities IC_{50} (nM)[a]	
		BRD4 BD1	BRD4 BD2
6	H	49.5±10.3	2479±170
12	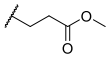	365.3±17.3	3690±145
JQ1[b]	---	62.57±5.83	39.09±10.35

[a] IC_{50} values were obtained from two separate experiments; [b] Used as a positive control.

To explore the interaction with proteins, we predicted the binding mode of compound **6** with BRD4 BD1 (**Figure 2C**). The binding conformation of the 1-methylbenzo[*cd*]indol-2(1*H*)-one moiety to Asn140 of the KAc pocket interacts with key hydrogen bonds, consistent with similar reported conformations[27]. Additional hydrogen bonding interactions are formed between the oxygen atom of the sulfonamide and the WPF water molecule. It is a significant difference that the para position of the ortho-methoxyphenyl group of compound **6** points to the Asp144 residue, and the ortho-methoxy group points to Leu92 (**Figure 2C**). This is the key to highlighting the selective binding of BD1 over BD2. The steric effect was performed between the para-position of the methoxy group on the benzene ring and the imidazole of His437 on BD2. Obviously, the binding to BD2 is unfavorable with AlphaScreen. The 4-position of 1-methylbenzo[*cd*]indol-2(1*H*)-one is in the BC loop solvent region and has a very large space. As

show selectivity of compound **12**. Therefore, the 4-position of 1-methylbenzo[*cd*]indol-2(1*H*)-one is suitable for the introduction of a pharmacodynamic fragment having the characteristics of PROTAC.

Our model of **6** docking (**Figure 2**C) with BRD4 BD1 protein suggested that the 4-position of the 1-methylbenzo[*cd*]indole-2(1*H*)-ketone core was exposed to the solvent environment adjacent to the BC loop, making it a suitable site to link to a ligand

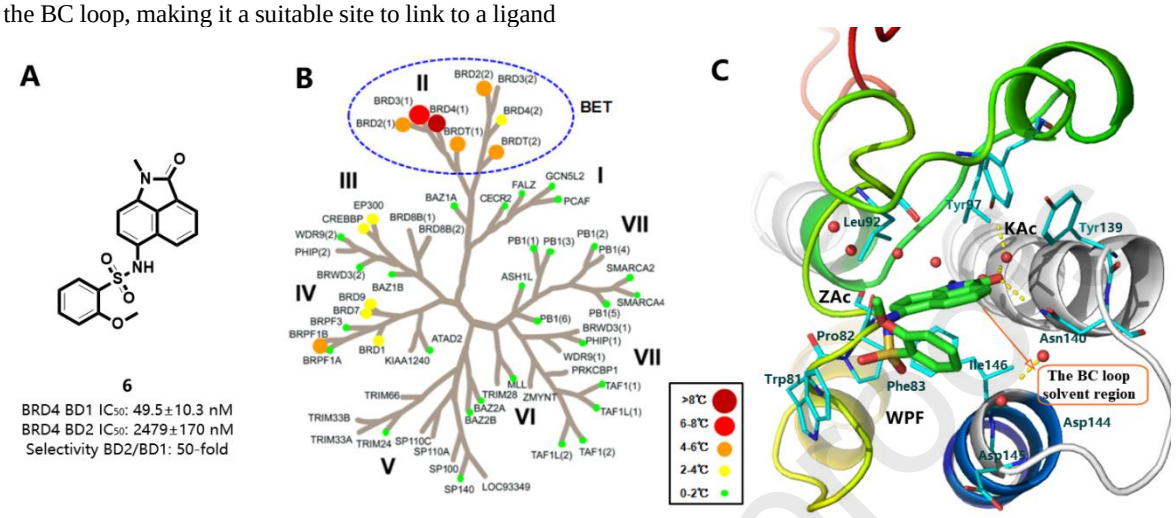

Figure 2. (A) Structure of selective-BD1 BET inhibitor **6** and its protein activities. (B) The bromodomains selectivity profile of **6** was shown by the bromodomains family tree vs. 48 bromodomains at 10 μM. Heat map shows the relative ΔTm values. Red indicates large ΔTm, and green indicates small ΔTm. (c) Binding mode analysis of compound **6** with BRD4 BD1 protein (protein shown as cartoon, PDB code 3MXF).

We first synthesized compound **13-17** as a potential BET degrading agent, carrying the propionic acid group of intermediate compound (the 4 position of compound **6** was replaced by a propyl group) and connecting the C4 atom of the isoindolin ring of thalidomide through a different carbon chain (**Figure 3**A). BET degraders had been reported to be sensitive to most leukemia cell lines such as MV4-11 and Molm-13. Therefore, we evaluated the antiproliferative activity of the designed BET protein degradation against these two cell lines (**Figure 3B-C**). As a control, we also evaluated the IC_{50} values of compound **6** against MV4-11 and Molm-13 (0.370 μM and 3.369 μM, respectively)

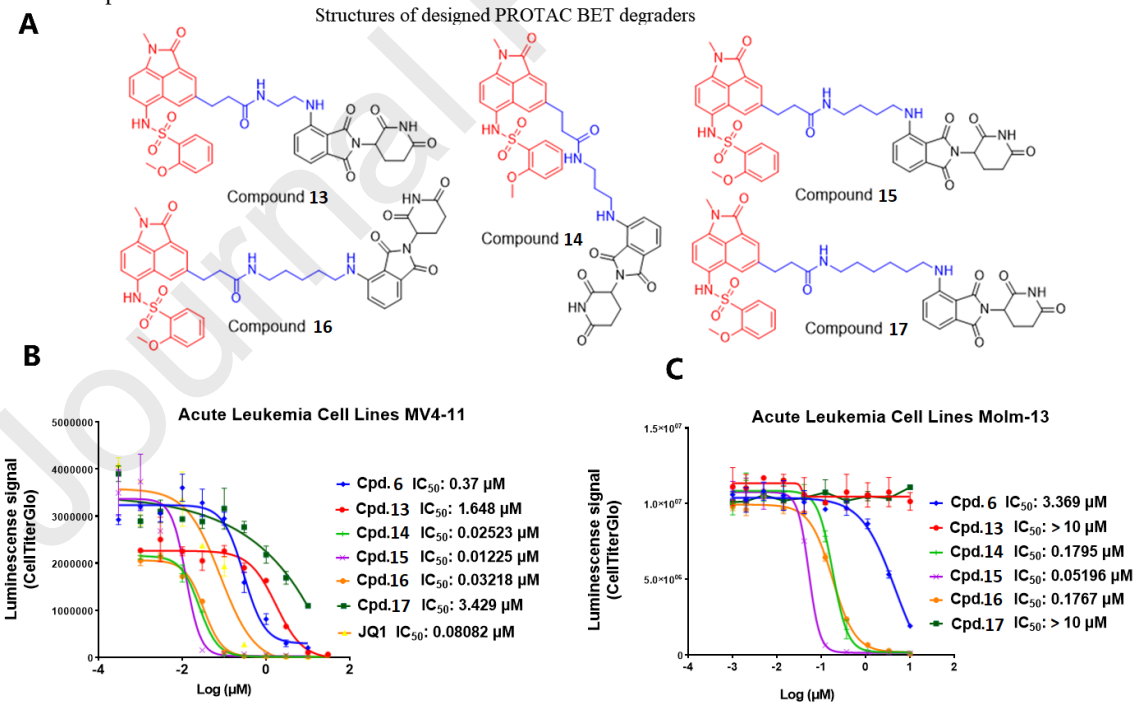

Figure 3. Structure and antiproliferative activity of designed PROTAC BET degraders: (A) Chemical structure designed PROTAC BET degraders (red shown as BET inhibitor, blue shown as linker and black shown as Cereblon inhibitor); (B-C) MV4-11 and Molm-13 cells treated with PROTACs and their corresponding BET targeting ligands for 48 h prior to quantitation of cell viability.

There are many factors affecting the efficiency of PROTAC molecular degradation, including protein ligand affinity, ligand type of E-ubiquitinated ligase, site of linker, length and type of linker, and overall physical and chemical properties of the molecule. The BET proteins are a "reader" key nuclear protein involved in gene transcription. The James E. Bradner team[29] identified the relationship between their compound degradation ability and treatment time. **Figure 3B-C** shows that the length of

degr d to them, the carbon chain length of 7 to 9 carbon chain length is superior in two leukemia cell lines (**14**, **15** and **16** in **Figure 3**). Compounds **14**, **15** and **16** are performed better anti-proliferation activity with IC_{50} values of 25.23 nM, 12.25 nM and 32.18 nM for MV4-11 cells, respectively. Simultaneously, **15** has IC_{50} values of 51.96 nM against Molm-13 cell lines. In order to examine treatment time, we investigated the degradation efficiency-time dependence. First, we selected compounds **15** with better anti-proliferation activity with IC_{50} values of 12.25 nM for MV4-11 accurately identify the appropriate treatment time. We designed six different time gradients to further determine the degradation-effect relationship of the degradation agent (**Figure. 4A-B**). Treatment of MV4-11 cells with compound **15** for 1 h, 2 h and 4 h failed to show BRD4 degradation at 100 nM. When treatment time of ≥ 8 hours with compound **15** at a concentration of 100 nM, the BRD4 protein was reduced very efficiently. Therefore, during the subsequent western blotting analysis, the incubation time of the experimental design compounds was greater than 8 h.

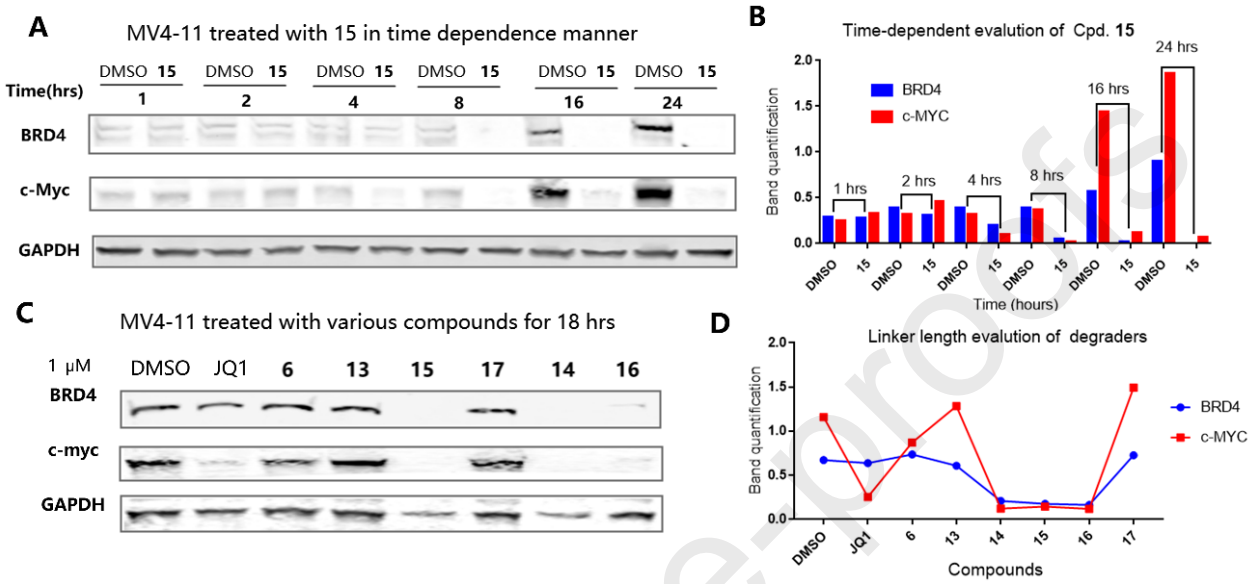

Figure 4. Western blotting analysis of BRD4 proteins and c-Myc in MV4-11. (A-B) Immunoblot for BRD4, c-Myc and GAPDH after a 1 hours, 2 hours, 4 hours, 8 hours, 16 hours, or 24 hours of treatment with DMSO and **15** (1 μM) in MV4-11 and quantified relative to GAPDH. (C-D) Immunoblot for BRD4, c-Myc and GAPDH after a 18-hour treatment with DMSO, **13-17** (1 μM), JQ1(**1**) and **6** (1 μM) in MV4-11 cells and quantified relative to GAPDH.

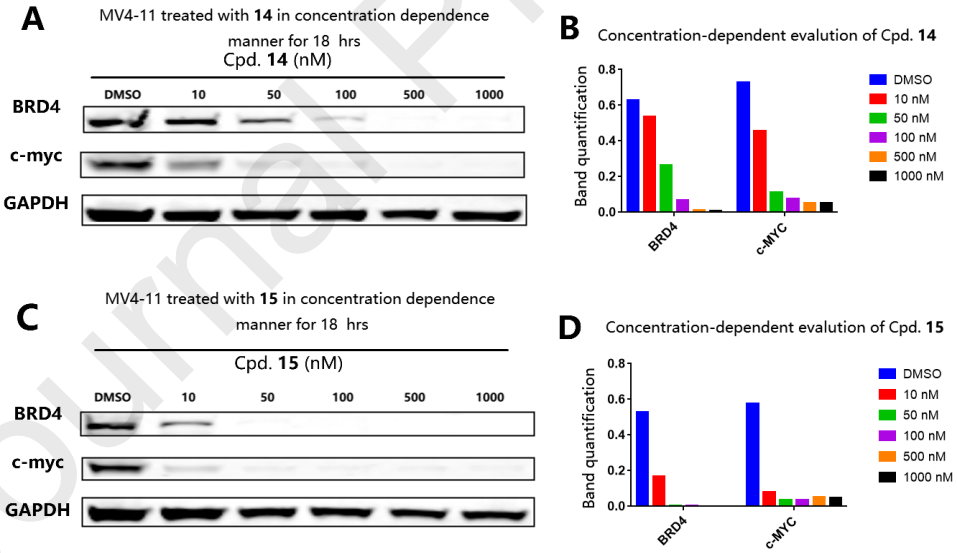

Figure 5. Western blotting analysis of BRD4 proteins and c-Myc in MV4-11 leukemia cells treated with BET degrader **14** and **15.** (A-B) Immunoblot for BRD4, c-Myc and GAPDH after treatment with **14** for 18 hours at the indicated concentration gradients (10 nM, 50 nM, 100 nM, 500 nM or 1000 nM), respectively and quantified relative to GAPDH. (C-D) Immunoblot for BRD4, c-Myc and GAPDH after treatment with **15** for 18 hours at the indicated concentration gradients (10 nM, 50 nM, 100 nM, 500 nM or 1000 nM), respectively and quantified relative to GAPDH.

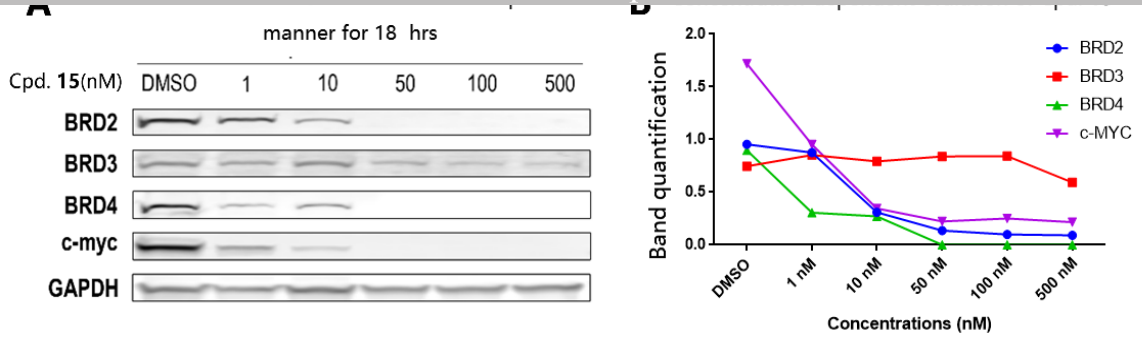

Figure 6. Western blotting analysis of **15**: Immunoblot for BRD4, BRD3, BRD2 and c-Myc in MV4-11 leukemia cells treated with BET degrader **15** for 18 hours at the indicated concentration gradients (1 nM, 10 nM, 50 nM, 100 nM or 500 nM), respectively (A) and quantified relative to GAPDH (B).

The length of the linker is a very important factor. Therefore, we designed compounds to to find the optimal length of linker. Consistent with result of **Figure 4C-D**, **1**((+)-JQ1) and **6** are competitive BET inhibitors that down-regulate the expression of the downstream Myc gene without altering the BRD4 protein. Compound **13** with a short linker failed to reduce the BRD4 protein, consistent with its cell activity. Compared to compound **13, c**ompound **14** was designed to add a carbon, whose cell activity increased 65-fold over **13** and the degradation activity was also greatly enhanced. We found that compounds **14-16** with suitable length linker are excellent in both anti-tumor cell proliferation level and its western blotting analysis molecular level. Since the linker was too long, the IC_{50} of compound **17** against MV4-11 was reduced to 3429 nM. Its cell activity was reduced by more than 100-fold compared to compound **14-16**. In summary, the length of linker in the range of 8-10 atoms length can be very efficient in its degradation efficiency. Among them, compound **15** with a 9 atoms length linker, is the best.

To further study the concentration dependence manner, compounds **14** and **15** with different concentration gradients were set up to investigate the degradation capacity of BRD4 protein (**Figure 5**). First, BRD4 protein was gradually degraded and c-MYC was down-regulated in MV4-11 cells at a treatment concentration of compound **14** of 50 nM for 18 h. As the concentration of compound **14** increased to 500 nM, the gray scale of the BRD4 protein band almost completely disappeared consistent with the background. Desirably, the BRD4 protein was degraded by treatment with compound **15** only at a concentration of 10 nM. Complete degradation of the BRD4 protein can be achieved at a concentration of 50 nM.

To confirm degradation activities of compound **15** basing on the selective-BD1 BET inhibitor, we examined the impact of BET proteins degradation and c-Myc levels. Interestingly, **Figure 6** showed that compound **15** performed depletion selectivity for BRD4 and BRD2 over BRD3, with good selectivity intra-BET proteins selectivity. The selectivity of compound **15** reduces the risk of potential toxicity and off-target effects. It is very difficult that degraders acquire degradation activities profiles due to the technical characteristics of PROTACS technology. Therefore, the results of homologous protein selection are very necessary and meaningful.

Encouraged by the efficient protein degradation efficiency of compound **15** and excellent blood tumor cell activity, we submitted **15** to the Developmental Therapeutics Program at NCI (http://dtp.nci.nih.gov) to test their cell activity against the NCI 60 cancer cell lines. Compound **15** exhibit potent inhibit activity on hematological tumors and solid tumors (**Table 2** and **Figure S2** in Supporting Information).

Table 2. The IG_{50} value of **15** against the NCI60 cancer cell lines

Panel	Cell line	GI_{50} (μM) [a]	Panel	Cell line	GI_{50} (μM)
Leukemia	CCRF-CEM	0.028	Melanoma	LOX IMVI	3.97
	HL-60(TB)	0.022		MALME-3M	0.161
	K-562	0.422		M14	0.937
	MOLT-4	0.031		MDA-MB-435	0.819
	RPMI-8226	0.683		SK-MEL-2	1.12
	SR	0.122		SK-MEL-5	1.21
Non-Small Cell Lung Cancer	A549/ATCC	5.26		SK-MEL-28	0.891
	EKVX	7.48		UACC-257	ND. [b]
	HOP-62	0.416		UACC-62	5.45
	HOP-92	0.026	Ovarian Cancer	IGROV1	0.145
	NCI-H226	0.456		OVCAR-3	1.83
	NCI-H23	37.5		OVCAR-4	0.259
	NCI-H322M	0.355		OVCAR-5	2.74
	NCI-H460	ND.		OVCAR-8	0.36
	NCI-H522	2.74		NCI/ADR-RES	ND.
Colon Cancer	COLO 205	0.495		SK-OV-3	1.63
	HCC-2998	0.316	Breast Cancer	MCF7	0.303
	HCT-116	3.66		MDA-MB-231	0.032
	HCT-15	ND.		HS 578T	0.186
	HT29	3.77		BT-549	0.078
	SW-620	0.675		T-47D	0.034
	KM12	0.249		MDA-MB-468	0.020
CNS Cancer	SF-268	0.366	Renal Cancer	786-0	2.11
	SF-295	3.22		A498	ND.
	SF-539	0.752		ACHN	ND.
	SNB-19	0.475		CAKI-1	2.63
	SNB-75	0.089		RXF 393	0.864
	U251	ND.		SN12C	0.447
Prostate Cancer	PC-3	0.248		TK-10	0.895
	DU-145	5.91		UO-31	ND.

[a] GI_{50} Growth inhibition of 50 %: calculated from $[(T_i-T_z)/(C-T_z)] \times 100 = 50$;
[b] not tested

From **Table 2**, compound **15** also exhibited excellent anti-proliferative activity in 6 leukemia cell lines of NCI. Among them, the GI_{50} values of the three leukemia cell lines were lower than 50 nM (GI_{50} is the concentration of test drug where $100 \times [(T_i-T_z)/(C-T_z)] = 50$, the growth inhibitory power of the test com

Table 3. The IC_{50} value of **15** against multiple cancer cell lines

Panel	Cell line	IC_{50} (μM)	Panel	Cell line	IC_{50} (μM)
Leukemia	MV-4-11	0.009797	Colon cancer	colo-205	0.1557
	RPMI8226	0.4395		DU145	3.66
Melanoma	A375	2.435	Thyroid[a]	TT	0.03745
Prostate Cancer	22RV1	0.081	Non-Small Cell Lung Cancer	A549	13.74
	LNCap clone FGC	0.62		H1975	0.4588
	LNCap	0.9095		HCC827	0.5802
	PC-3	0.932		H1650	1.332
	Vcap	0.2504		H358	1.381

[a] Human thyroid cancer cell line.

Excitingly, compound **15** also showed outstanding anti-cell proliferation activity against multiple solid tumor cell lines. Mainly concentrated in breast cancer cell lines, the GI_{50} values of triple-negative cell lines MDA-MB-231 and MDA-MB-468 were 32 nM and 20 nM, respectively. Other breast cancer cell lines have GI_{50} values less than 0.5 μM. In addition, other various solid tumor cell lines can be inhibited by compound **15**, such as GI_{50} values of 26 nM and 89 nM for non-small cell lung cancer HOP-92 and CNS cancer SNB-75, respectively. Furthermore, we further increased the cancer cell spectrum. As shown in **Table 3** and **Figure S3** in Supporting Information, the cell activity results showed that the compound **15** had good anti-proliferation activity including prostate Cancer (22RV1 IC_{50}: 0.081 μM), colon cancer(colo-205 IC_{50}: 0.1557μM) and thyroid cancer(TT IC_{50}: 0.037451 μM).

research aspects of BET protein degraders. For the great majority of the cell lines, LC_{50} (which signifies a cytotoxic effect, is the concentration of drug where $[(T_i\text{-}T_z)/T_z] \times 100 = 50$, the control optical density is not used in the calculation of LC_{50}) was >100 μM (**Figure S2** in Supporting Information). It is indirectly indicated that the compound **15** with selective degradation for BRD4 and BRD2 over BRD3 has good targeting and safety, since the data aggregates specific cell lines, rather than extensive inhibitory activity against all cell lines.

Subsequently, we used flow cytometry to study the ability of **15** to induce MV4-11 apoptosis lines, and found that **15** has a strong induction effect in a concentration-dependent manner (**Figure 7A** and **Figure S4**). In the MV4-11 cell line for 24 hours, compared to the DMSO, it induced >80% of cells to undergo apoptosis treatment at concentrations as low as 100 nM. The induction apoptosis rate of negative control **6** was 86.07% at a high concentration of 10 μM for 24 hours. Meanwhile, when the treatment time was extended to 48 hours, the apoptosis rate of **15** significantly increased to 86.86% at a concentration as low as 30 nM (**Figure 7B** and **Figure S4**).

In addition, we used flow cytometry analysis (**Figure 7C** and **Figure S5**) to investigate the effect of **15** on cell cycle in MV4-11. Compound **15** was found to block the cell cycle at 100 nM (71.37% of G1 phase) comparable to compound **6** at 10 μM. Significantly higher than the G1 phase of the control was 59.66%. As the concentration increases ≥ 300 nM, the tumor cells are completely blocked in the G1 phase.

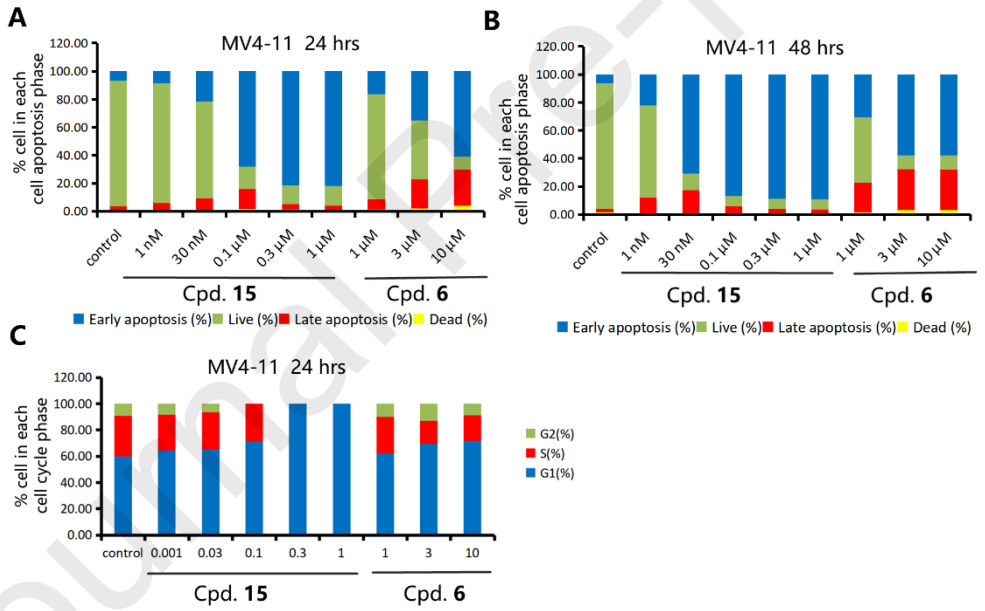

Figure 7. Flow cytometry analysis of apoptosis induction and cell cycle arrest by degrader **15** and inhibitor **6** in MV4-11 leukemia cells. (A-B), different concentrations of gradient degrading agent **15** and inhibitor **6**, the drug treatment time was 24 h (A) and 48 h (B) of apoptosis induction, respectively. (C), different concentrations of gradient degrading agent **15** and inhibitor **6**, the drug treatment time was 24 h of cell cycle arrest.

3. Chemistry

The synthesis of the BET inhibitor **24** is shown in **Scheme 1**. Starting from inexpensively available 1,8-Naphthalic anhydride, intermediate **18** was synthesized through halogenation reaction with bromine and silver sulfate in concentrated sulfuric acid. Two crucial steps, a nucleophilic substitution reaction sulfonylation and strong base decarboxylation, were carried out one pot, showing moderate yields obtained **19**. Subsequently, **22** was synthesized through a three-step reaction including methylation with methyl iodide, nitrification under acetic acid-nitric acid conditions and Heck coupling reaction with methyl acrylate. The intermediates were reduced to hydrogenation used for a next step. Finally, the title compound **24** was prepared with 2-methoxybenzenesulfonyl chloride. The synthesis of the BET Degraders **13-17** were shown in **Scheme 2**. Starting from 4-fluoroisobenzofuran-1,3-dione and 3-aminopiperidine-2,6-dione hydrochloride, the intermediate **25** was synthesized under heating with acetic acid and acetic acid. Subsequently, **29a-29e** were prepared by two steps including nucleophilic amination and trifluoroacetic acid Boc reaction. Finally, the title compounds **13-17** were obtained by condensation reaction of the intermediates **29a-29e** with **24**, respectively.

Scheme 2. Compound **24**

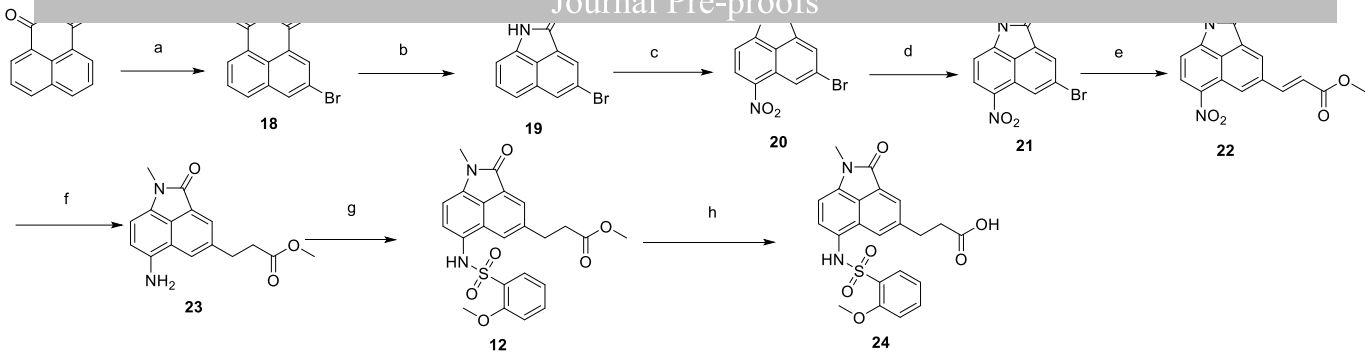

Reagents and conditions: (a) Br_2, H_2SO_4, Ag_2SO_4, 60 °C; (b) i: NH_2OH HCl, TsCl, pyridine, 90 °C; ii:NaOH, HCl, EtOH, H_2O; (c) HNO_3, AcOH, 60 °C; (d) CH_3I, 60% NaH, DMF; (e) methyl acrylate, $Pd(PPh_3)_4$, 1,4-dioxane, N_2, 80 °C; (f) Pd/C, H_2, THF, MeOH, r.t.; (g) 2-methoxybenzenesulfonyl chloride, pyridine, DCM, r.t; (h) NaOH, HCl, H_2O, r.t.

Scheme 2. Compounds **13-17.**

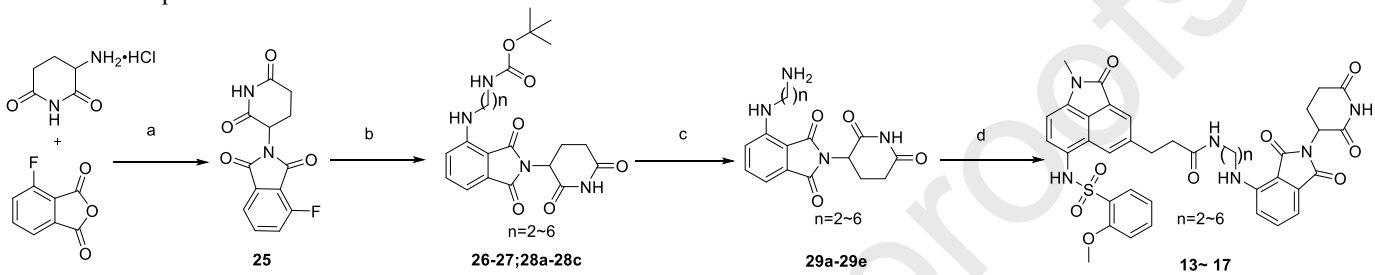

[a]Reaction conditions: (a) AcONa, AcOH, 105 °C; (b) Proper amine, 1,4-dioxane, N_2, 80 °C; (c) TFA, DCM, rt. (d) Compound **24**, HATU, DIPEA, DMF, rt..

4. Conclusion

We describe a BET inhibitor, which binds to BRD4 BD1 with an affinity of 50-fold over BRD4 BD2 and is selected for binding to the BET family compared to other Bromodomains. The binding conformation of compound **6** to BRD4(1) protein was described, and novel PROTAC degraders of BET proteins were designed by linking the Thalidomide with a linker. The structure-activity relationship between length of the linker and anti-tumor activity was explored and summarized. When the linker is 8 carbon-based distances, the degrader **15** has an efficient inhibition of blood tumor and solid tumor cell growth in cell profiles. In addition, compound **15** exhibited a very low cytotoxic effect in the NCI60 cell lines. The study found that BRD4 proteins in MV4-11 was completely degraded by compound **15** for 8 h and dose-dependent tests showed that compound **15** was still effective as low as 10 nM. Besides, this molecule could induce apoptosis and cell cycle arrest. We have demonstrated that BET ligands with selectivity for bromodomains could be designed to achieve selective degraders of intra-BET proteins, providing insights into the design of selective degradation intra-BET proteins and low toxicity degraders. More generally, we provide efficiently novel PROTAC degraders of BRD4 and BRD2 proteins as a promising drug for the treatment of cancer.

5. Materials and methods

5.1. Chemistry General Methods.

Unless otherwise specified, reagents were purchased from commercial suppliers and used without further purification. Melting points were determined by X-4 digital display micro-melting point apparatus (Beijing Tech Instrument Co., Ltd.); NMR spectra were recorded on Bruker AVANCE AV-600 spectrometer (400 or 300 MHz for 1H, 200 or 150 MHz for ^{13}C); Mass spectra were obtained on the Agilent 1100 LC / MSD mass spectrometer (Agilent, USA) and Q-tofmicro MS (micromass company). The HPLC traces of title compounds were provided on the Agilent 1260 HPLC (Agilent, USA). All reactions were monitored by TLC (Merck Kieselgel GF254) and spots were visualized with UV light or iodine.

5.1.1 General Procedure for Synthesis of Compound **2** in **Scheme 1**.

5.1.1.1

5-bromo-1*H*,3*H*-benzo[*de*]isochromene-1,3-dione (18). To a solution of 1,8-Naphthalic anhydride (10.0 g, 50.5 mmol, 1 equiv) and silver sulfate (7.9 g, 25.25 mmol, 0.50 equiv) in concentrated sulfuric acid (200 mL) were stirred at room temperature. Bromine (3.2 mL, 63.0 mmol, 1.26 equiv) was added over 30 min, and then heated to 60 °C for 8-10 h, before cooling back to 20 °C. The solid silver bromide by product was filtered off at a water pump to give a clear orange solution. This mixture reaction was added dropwise to ice water mixture (1 L). An off-white solid precipitates was filtered. The filter cake was washed once by displacement with water (50 mL) and twice with cold ethanol (100 mL each) and dried in vacuo at 60 °C to constant weight to yield the title compound **18** as white solid (12.54 g, 45.5 mmol, 90% yield). $[M+H]^+$: 277.1. ^1H NMR (300 MHz, DMSO-d_6) δ 8.83 (s, 1H), 8.57 – 8.44 (m, 3H), 7.93 (q, J = 9.4, 8.6 Hz, 1H).

5.1.1.2

4-bromobenzo[*cd*]indol-2(1*H*)-one (19). To a solution of 5-bromo-1*H*,3*H*-benzo[*de*]isochromene-1,3-dione **18** (10 g, 36.2 mmol, 1 equiv) and hydroxylamine hydrochloride (2.5 g, 36.2 mmol, 1 equiv) in pyridine (70 mL) was conducted under reflux for 2 h, followed by cooling to 80 °C. Then ptoluenesulfonyl chloride (13.8 g, 72.4 mmol, 2 equiv) was added to the reaction system. After addition, the temperature was raised and the reaction was carried out under reflux for 2 h, followed by cooling. The reaction mixture was poured into 0.40 L of water and stirred to precipitate crystals, which were collected by filtration. The crystals were transferred to a beaker and washed successively with 0.5 L of a $NaHCO_3$ aqueous solution and 0.5 L of water, followed by filtration. The crystals were washed with water and dried to give an intermediate for further reaction. The whole amount of the

inte… …l-2-oxo-1,2-dihydrobenzo[cd]indol-4-yl)propanoate (12).

reactor and stirred. Then 130 ml of a 1.4 mol/L aqueous solution of NaOH was added dropwise to the mixture. Thereafter, the mixture was heated to refluxing temperature, at which the reaction was carried out for 3 h while distilling off ethanol. After completion of the reaction, the reaction mixture was cooled to 75 °C, and 60 ml of concentrated HCl was added dropwise. In the meantime, crystals precipitated at 60 °C. After completion of the dropwise addition, the mixture was further cooled. The precipitated crystals were collected by filtration, washed with ion-exchanged water, and dried to give the title compound **19** as white solid (2.76 g, 11.22 mmol, 31% yield). $[M+H]^+$: 248.1. ^1H NMR (300 MHz, DMSO-d_6) δ 10.92 (s, 1H), 8.44 (s, 1H), 8.10 (s, 1H), 7.58 (d, J = 3.5 Hz, 2H), 7.01 (dd, J = 5.9, 1.8 Hz, 1H).

5.1.1.3

4-bromo-6-nitrobenzo[*cd*]indol-2(1*H*)-one (20). To a solution of 4-bromo-6-nitrobenzo[*cd*]indol-2(1*H*)-one **19** (7 g, 28.5 mmol) in AcOH (15 mL) was added 69% HNO_3 (2 mL, 42.75 mmol) heat to 50 °C - 65 °C. The mixture reaction was stirred for 4 h. When TLC analysis showed complete conversion of the starting material, the reaction mixture was poured into water filtrated through Cellit and the filtrate was concentrated in vacuum. The crude product was purified by silica gel column chromatography (PE/DCM) to yielded the title compound **20** as yellow solid (6.9 g, 23.65 mmol, 83% yield). $[M+H]^+$: 293.1. ^1H NMR (300 MHz, DMSO-d_6) δ 8.91 (s, 1H), 8.67 (d, J = 8.1 Hz, 1H), 8.31 (s, 1H), 7.32 (d, J = 8.1 Hz, 1H), 3.38 (s, 3H).

5.1.1.4

4-bromo-1-methyl-6-nitrobenzo[*cd*]indol-2(1*H*)-one (21). To a solution of 4-bromo-1-methyl-6-nitrobenzo[*cd*]indol-2(1*H*)-one **20** (6.5 g, 22.26 mmol, 1 equiv) in anhydrous DMF (100 mL) was stirred at 0 °C. The solution was added 60% NaH (1.34 g, 33.35 mmol, 1.5 equiv) in 3 batches and stirring for 30 minutes. Methyl iodide (2.06 mL, 33.35 mmol, 1 equiv) was added dropwise to the mixture, and the whole was stirred at room temperature for 3 h and then was poured into ice water. This mixture was extracted with AcOEt. The organic layer was washed with H_2O and brine for 4 times, dried ($MgSO_4$), concentrated and purified by silica gel column chromatography to afford the title compound **21** as yellow solid (5.52 g, 18.04 mmol, 81% yield). $[M+H]^+$: 306.9. ^1H NMR (300 MHz, DMSO-d_6) δ 8.91 (s, 1H), 8.67 (d, J = 8.1 Hz, 1H), 8.31 (s, 1H), 7.32 (d, J = 8.1 Hz, 1H), 3.38 (s, 3H).

5.1.1.4

Methyl(*E*)-3-(1-methyl-6-nitro-2-oxo-1,2-dihydrobenzo[*cd*]indol-4-yl)acrylate (22). To mixture of 4-bromo-1-methyl-6-nitrobenzo[*cd*]indol-2(1*H*)-one **20** (500 mg, 1.63 mmol, 1 equiv), $Pd(AcO)_2$ (18 mg, 0.08 mmol, 0.05 equiv), tri-*o*-tolylphosphane (49 mg, 0.16 mmol, 0.1 equiv) and K_2CO_3 (675 mg, 4.88 mmol, 3 equiv) was dissolved in anhydrous 1,4-dioxane. The reaction mixture was added methyl acrylate (293 mL, 4.88 mmol, 2 equiv). The reaction system was exchanged by N_2, then, heated to 80 °C for 7 h. When TLC analysis showed complete conversion of the starting material, the mixture was extracted with AcOEt and water. The organic layer was washed with H_2O and brine, dried ($MgSO_4$), concentrated and purified by silica gel column chromatography to afford the title compound **22** as yellow solid (381 mg, 1.22 mmol,75% yield). $[M+H]^+$: 313.2. ^1H NMR (300 MHz, DMSO-d_6) δ 8.96 (s, 1H), 8.70 – 8.56 (m, 2H), 7.98 (d, J = 16.1 Hz, 1H), 7.30 (d, J = 8.1 Hz, 1H), 6.98 (d, J = 16.1 Hz, 1H), 3.78 (s, 3H), 3.40 (s, 3H).

5.1.1.5

solution of compounds **22** (380 mg, 1.21 mmol, 1 equiv) in 20 mL EtOH was added 100 mg the Raney-Nickel catalyst (with about 50% water). The mixture reaction was flushed thrice with argon then thrice with hydrogen. The flask was charged with hydrogen gas, and reaction mixture was left to stir for 5 h. The reaction was completely detected by LTC. The reaction mixture was filtered through celite, and filtered and evaporated. The maroon rude was used as a next step. To a solution of the maroon rude in 20 mL DCM was added 2-methoxybenzenesulfonyl chloride (301 mg, 1.46 mmol, 1.2 equiv) and pyridine 0.5 mL. The reaction solution was stirred at room temperature overnight. The reaction was completed by TLC and then concentrated. Purification by column chromatography (30% EA/PE) yielded the title compound **12** as yellow solid (287. mg, 0.63 mmol, 53% yield). m.p 103-105 °C. HPLC analysis: retention time = 3.359 min; peak area, 97.75%. ^1H NMR (300 MHz, Chloroform-*d*) δ 7.99 (s, 1H), 7.90 (s, 1H), 7.68 (dd, J = 7.7, 1.7 Hz, 1H), 7.51 (dd, J = 15.9, 1.8 Hz, 1H), 7.16 (s, 1H), 7.10 (d, J = 7.8 Hz, 2H), 6.95 (t, J = 7.7 Hz, 1H), 6.63 (d, J = 7.5 Hz, 1H), 4.13 (s, 3H), 3.68 (s, 3H), 3.34 (s, 3H), 3.19 (t, J = 7.6 Hz, 2H), 2.71 (t, J = 7.6 Hz, 2H). HRMS-EI *m/z* $[M+H]^+$ calcd for $C_{23}H_{23}N_2O_6S^+$: 455.1271, found: 455.1271.

5.1.1.6

3-(6-((2-methoxyphenyl)sulfonamido)-1-methyl-2-oxo-1,2-dihydrobenzo[cd]indol-4-yl)propanoic acid (24). To a solution of compounds **12** (250 mg, 0.55 mmol, 1 equiv) in 15mL MeOH was added 1 mL sodium hydroxide solution (2 mmol/mL). The reaction solution was stirred at room temperature for 1 hour. The reaction was completely detected by LTC. The methanol in the reaction was distilled off under reduced pressure. This mixture was extracted with AcOEt (50 mL) and water (30 mL × 3). The aqueous layer was acidified with a solution of 2N HCl (1.5 mL) and extracted with methylene chloride. The organic layer was dried over $MgSO_4$ and concentrated under vacuum to give the title compound **24** as yellow solid (220 mg, 0.5 mmol, 91% yield) requiring no further purification.

*5.1.2 General Procedure for Synthesis of Compound **13-17**.*

5.1.2.1

2-(2,6-dioxopiperidin-3-yl)-4-fluoroisoindoline-1,3-dione (25). To a solution of 4-fluoroisobenzofuran-1,3-dione (2 g, 12.04 mmol, 1 equiv) in 20 mL AcOH was added 3-aminopiperidine-2,6-dione hydrochloride (2.18 g, 13.24 mmol, 1.1 equiv) and AcOK (2.36 g, 24.08 mmol, 2 equiv). The solution was then stirred at 60 °C for 12 h. After cooling to room temperature, the solution was extracted with AcOEt. The organic layer was washed with H_2O and brine for 4 times, dried ($MgSO_4$), concentrated and purified by silica gel column chromatography to afford the title compound **25** as a white solid (2.13 g, 7.71 mmol, 64% yield). $[M+H]^+$: 277.2. ^1H NMR (300 MHz, DMSO-d_6) δ 11.16 (s, 1H), 7.95 (td, J = 7.8, 4.4 Hz, 1H), 7.84 – 7.68 (m, 2H), 5.17 (dd, J = 12.9, 5.4 Hz, 1H), 2.99 – 2.81 (m, 1H), 2.67 – 2.52 (m, 2H), 2.15 – 2.00 (m, 1H).

5.1.2.2

***tert*-butyl(2-((2-(2,6-dioxopiperidin-3-yl)-1,3-dioxoisoindolin-4-yl)amino)ethyl)carbamate (26).** To a solution of 4-fluoroisobenzofuran-1,3-dione (300 mg, 1.09 mmol, 1 equiv) in 15 mL anhydrous 1,4-dioxane was added *tert*-butyl (2-aminoethyl)carbamate (226 mg, 1.41 mmol 1.3 equiv). The solution was then stirred at 80 °C for 12 h. After cooling to room temperature, the solution was extracted with AcOEt (50 mL × 3). The organic layer was washed with H_2O and brine for 4 times, dried ($MgSO_4$), concentrated and purified by silica gel column

chro… …d at
yellow solid (199 mg, 0.48 mmol, 44% yield). [M+H]$^+$: 417.2. ^{1}H NMR (300 MHz, Chloroform-*d*) δ 8.32 (s, 1H), 7.50 (dd, *J* = 8.5, 7.1 Hz, 1H), 7.11 (d, *J* = 7.1 Hz, 1H), 6.98 (d, *J* = 8.5 Hz, 1H), 6.40 (s, 1H), 4.93 (q, *J* = 5.3 Hz, 2H), 3.50 – 3.30 (m, 4H), 2.94 – 2.70 (m, 3H), 2.12 (dt, *J* = 8.8, 3.1 Hz, 1H), 1.44 (s, 9H).

5.1.2.3

***tert*-butyl(3-((2-(2,6-dioxopiperidin-3-yl)-1,3-dioxoisoindolin-4-yl)amino)propyl)carbamate (27).** Compound **27** was prepared according to **26** on 1.09 mmol scale, starting from *tert*-butyl (3-aminopropyl)carbamate and **25**. Purification by column chromatography (EA/PE) yielded the title compound **27** as a light yellow solid (182 mg, 0.42 mmol, 39% yield). [M+H]$^+$: 431.3. ^{1}H NMR (300 MHz, Chloroform-*d*) δ 8.59 (s, 1H), 7.49 (t, *J* = 7.9 Hz, 1H), 7.09 (d, *J* = 7.2 Hz, 1H), 6.89 (d, *J* = 8.5 Hz, 1H), 6.34 (s, 1H), 4.95 (t, *J* = 5.9 Hz, 1H), 4.81 (s, 1H), 3.29 (dt, *J* = 29.0, 6.7 Hz, 4H), 2.96 – 2.63 (m, 3H), 2.19 – 2.05 (m, 1H), 1.85 (p, *J* = 7.1 Hz, 2H), 1.46 (s, 9H).

5.1.2.4

tert-butyl(4-((2-(2,6-dioxopiperidin-3-yl)-1,3-dioxoisoindolin-4-yl)amino)butyl)carbamate (28a). Compound **28a** was prepared according to **26** on 1.09 mmol scale, starting from *tert*-butyl (4-aminobutyl)carbamate and **25**. Purification by column chromatography (EA/PE) yielded the title compound **28a** as a light yellow solid (248 mg, 0.57 mmol, 53% yield). [M+H]$^+$: 445.3. ^{1}H NMR (300 MHz, Chloroform-*d*) δ 8.36 (s, 1H), 7.53 – 7.45 (m, 1H), 7.09 (d, *J* = 7.1 Hz, 1H), 6.88 (d, *J* = 8.5 Hz, 1H), 6.24 (s, 1H), 4.92 (dd, *J* = 11.9, 5.4 Hz, 1H), 4.63 (s, 1H), 3.30 (t, *J* = 6.7 Hz, 2H), 3.17 (d, *J* = 6.2 Hz, 2H), 2.94 – 2.63 (m, 4H), 2.12 (dt, *J* = 8.9, 3.3 Hz, 1H), 1.77 – 1.50 (m, 5H).

5.1.2.5

tert-butyl(5-((2-(2,6-dioxopiperidin-3-yl)-1,3-dioxoisoindolin-4-yl)amino)pentyl)carbamate (28b). Compound **28b** was prepared according to **26** on 1.09 mmol scale, starting from *tert*-butyl (5-aminopentyl)carbamate and **25**. Purification by column chromatography (EA/PE) yielded the title compound **28b** as a light yellow solid (229 mg, 0.50 mmol, 46% yield). [M+H]$^+$: 459.23. ^{1}H NMR (300 MHz, Chloroform-*d*) δ 8.54 (s, 1H), 7.48 (dd, *J* = 8.6, 7.1 Hz, 1H), 7.08 (d, *J* = 7.1 Hz, 1H), 6.87 (d, *J* = 8.5 Hz, 1H), 6.24 (t, *J* = 5.6 Hz, 1H), 4.97 – 4.87 (m, 1H), 4.64 (s, 1H), 3.26 (q, *J* = 6.6 Hz, 2H), 3.13 (q, *J* = 6.6 Hz, 2H), 2.91 – 2.72 (m, 3H), 1.67 (q, *J* = 7.1 Hz, 2H), 1.57 – 1.49 (m, 2H), 1.44 (s, 9H), 1.26 (d, *J* = 3.5 Hz, 3H).

5.1.2.6

tert-butyl(6-((2-(2,6-dioxopiperidin-3-yl)-1,3-dioxoisoindolin-4-yl)amino)hexyl)carbamate (28c). Compound **18c** was prepared according to **26** on 1.09 mmol scale, starting from *tert*-butyl(6-aminohexyl)carbamate and **25**. Purification by column chromatography (EA/PE) yielded the title compound **28c** as a light yellow solid (240 mg, 0.51 mmol, 47% yield). [M+H]$^+$: 473.2. ^{1}H NMR (300 MHz, Chloroform-*d*) δ 8.53 (s, 1H), 7.48 (dd, *J* = 8.5, 7.1 Hz, 1H), 7.08 (d, *J* = 7.1 Hz, 1H), 6.87 (d, *J* = 8.6 Hz, 1H), 6.24 (t, *J* = 5.7 Hz, 1H), 4.92 (dd, *J* = 11.8, 5.4 Hz, 1H), 4.60 (s, 1H), 3.25 (q, *J* = 6.6 Hz, 2H), 3.10 (t, *J* = 6.8 Hz, 2H), 2.93 – 2.69 (m, 3H), 2.12 (dt, *J* = 8.8, 3.1 Hz, 1H), 1.65 (q, *J* = 7.2 Hz, 2H), 1.54 – 1.47 (m, 2H), 1.44 (s, 9H), 1.43 – 1.35 (m, 4H), 1.26 (d, *J* = 3.4 Hz, 1H).

5.1.2.7

***N*-(2-((2-(2,6-dioxopiperidin-3-yl)-1,3-dioxoisoindolin-4-yl)amino)ethyl)-3-(6-((2-methoxyphenyl)sulfonamido)-1-methyl-2-oxo-1,2-dihydrobenzo[*cd*]indol-4-yl)propanamide (13).** To a solution of compounds **26** (190 mg, 0.45 mmol, 1 equiv) … room temperature for 1 h. The reaction was completely detected by LTC. The trifluoroacetic acid in the solution was concentrated under reduced pressure by an oil pump. The light yellow rude (135 mg, 94% yield) was used as a next step. To a solution of light yellow rude (56 mg, 0.18 mmol, 1.3 equiv) in 20 mL anhydrous DMF was added **24** (60 mg, 0.136 mmol, 1 equiv), HATU (76 mg, 0.20 mmol, 1.5 equiv) and DIPEA (52 mg, 0.40 mmol, 3 equiv). The reaction was completed by TLC. The reaction solution was poured into water and extracted with AcOEt. The organic layer was washed with H_2O and brine for 4 times, dried ($MgSO_4$), concentrated and purified by silica gel column chromatography (EA/PE) to afford the title compound **13** as a light yellow solid (74 mg, 0.10 mmol, 74% yield). m.p 183-185 °C. HPLC analysis: retention time = 3.254 min; peak area, 98.47%. ^{1}H NMR (300 MHz, Chloroform-*d*) δ 8.82 (s, 1H), 8.06 (s, 1H), 7.84 (s, 1H), 7.65 (s, 2H), 7.49 (t, *J* = 7.9 Hz, 1H), 7.40 (t, *J* = 7.7 Hz, 1H), 7.05 (d, *J* = 7.6 Hz, 3H), 6.91 (t, *J* = 7.7 Hz, 1H), 6.78 (d, *J* = 8.5 Hz, 1H), 6.55 (d, *J* = 7.5 Hz, 1H), 6.22 (s, 2H), 4.97 (s, 1H), 4.09 (s, 3H), 3.45 (s, 2H), 3.28 (s, 3H), 3.31 -3.11 (m, 6H), 2.83 (dt, *J* = 22.3, 10.3 Hz, 4H), 2.58 (d, *J* = 7.7 Hz, 2H). HRMS-EI *m/z* [M+H] $^+$ calcd for $C_{37}H_{35}N_6O_9S^+$: 739.2181, found: 739.2175. ^{13}C NMR (101 MHz, Chloroform-*d*) δ 172.36 , 171.91 , 169.48 , 169.44 , 167.98 , 167.68 , 156.37 , 146.44 , 142.22 , 138.09 , 136.06 , 135.03 , 132.39 , 130.73 , 126.90 , 126.78 , 126.50 , 126.44 , 125.71 , 125.61 , 124.36 , 123.96 , 120.54 , 116.52 , 112.04 , 111.35 , 109.82 , 104.45 , 77.26 , 56.32 , 48.93 , 39.91 , 37.94 , 31.43 , 28.68 , 26.27 , 22.79 .

5.1.2.8

***N*-(3-((2-(2,6-dioxopiperidin-3-yl)-1,3-dioxoisoindolin-4-yl)amino)propyl)-3-(6-((2-methoxyphenyl)sulfonamido)-1-methyl-2-oxo-1,2-dihydrobenzo[*cd*]indol-4-yl)propanamide (14).** Compound **14** was prepared according to **13** in two steps, respectively, starting from **27** (180 mg, 0.42 mmol, 1 equiv) and **24** (60 mg, 0.136 mmol, 1 equiv). Purification by column chromatography (EA/PE) yielded the title compound **14** as a light yellow solid (66 mg, 0.088 mmol, 65% yield). m.p 161-163 °C. HPLC analysis: retention time = 3.317 min; peak area, 97.01%. ^{1}H NMR (300 MHz, Chloroform-*d*) δ 8.59 (s, 1H), 8.05 (s, 1H), 7.89 (s, 1H), 7.72 (s, 2H), 7.49 (t, *J* = 7.5 Hz, 1H), 7.43 – 7.38 (m, 1H), 7.16 – 6.99 (m, 3H), 6.91 (t, *J* = 7.6 Hz, 1H), 6.70 (d, *J* = 8.5 Hz, 1H), 6.60 (d, *J* = 7.6 Hz, 1H), 5.86 (s, 2H), 4.95 (s, 1H), 4.13 (s, 3H), 3.31 (s, 3H), 3.34 – 3.31 (m, 2H), 3.18 (d, *J* = 7.0 Hz, 2H), 3.08 (s, 2H), 2.89 – 2.72 (m, 4H), 2.59 (t, *J* = 7.2 Hz, 2H), 2.13 (d, *J* = 8.5 Hz, 2H). HRMS-EI *m/z* [M+H] $^+$ calcd for $C_{38}H_{37}N_6O_9S^+$: 753.2337, found: 753.2325. ^{13}C NMR (101 MHz, Chloroform-*d*) δ 172.48 , 171.78 , 169.43 , 169.35 , 168.06 , 167.65 , 156.37 , 146.44 , 142.18 , 138.10 , 136.08 , 135.03 , 132.40 , 130.74 , 126.96 , 126.79 , 126.56 , 126.46 , 125.74 , 125.68 , 124.38 , 124.00 , 120.57 , 116.52 , 112.06 , 111.39 , 109.87 , 104.53 , 77.25 , 56.35 , 48.93 , 39.98 , 37.97 , 32.44 , 31.43 , 28.67 , 26.31 , 22.80 .

5.1.2.9

***N*-(4-((2-(2,6-dioxopiperidin-3-yl)-1,3-dioxoisoindolin-4-yl)amino)butyl)-3-(6-((2-methoxyphenyl)sulfonamido)-1-methyl-2-oxo-1,2-dihydrobenzo[*cd*]indol-4-yl)propanamide (15).** Compound **15** was prepared according to **13** in two steps, respectively, starting from **28a** (240 mg, 0.56 mmol, 1 equiv) and **24** (60 mg, 0.136 mmol, 1 equiv). Purification by column chromatography (EA/PE) yielded the title compound **15** as a light yellow solid (69 mg, 0.092 mmol, 68% yield). m.p 155-157 °C. HPLC analysis: retention time = 2.734 min; peak area, 98.09%. ^{1}H NMR (300 MHz, Chloroform-*d*) δ 8.46 (s, 1H), 8.06 (s, 1H), 7.88 (s, 1H), 7.69 – 7.55 (m, 2H), 7.48 (q, *J* = 9.0, 8.6 Hz, 2H), 7.18 –

6.99 nM 6.57 (d, *J* = 7.5 Hz, 1H), 5.92 (s, 2H), 4.93 (s, 1H), 4.12 (s, 3H), 3.27 (s, 3H), 3.26 - 3.20 (m, 2H), 3.08 (s, 2H), 2.94 – 2.67 (m, 4H), 2.13 -2.09 (m, 2H). HRMS-EI *m/z* [M+H] $^{+}$ calcd for $C_{39}H_{39}N_6O_9S^+$: 767.2494, found: 767.2490. ^{13}C NMR (101 MHz, Chloroform-*d*) δ 171.57 , 171.37 , 169.56 , 168.81 , 167.97 , 167.68 , 156.32 , 146.92 , 142.46 , 138.53 , 136.18 , 135.04 , 132.44 , 130.72 , 126.92 , 126.81 , 126.50 , 126.44 , 126.06 , 125.77 , 124.42 , 124.22 , 120.66 , 116.73 , 112.18 , 111.41 , 109.78 , 104.20 , 77.26 , 56.51 , 48.90 , 42.46 , 39.34 , 38.20 , 31.43 , 29.28 , 28.81 , 26.47 , 22.82 .

5.1.2.10

N-(5-((2-(2,6-dioxopiperidin-3-yl)-1,3-dioxoisoindolin-4-yl)amino)pentyl)-3-(6-((2-methoxyphenyl)sulfonamido)-1-methyl-2-oxo-1,2-dihydrobenzo[cd]indol-4-yl)propanamide (16). Compound **15** was prepared according to **13** in two steps, respectively, starting from **28b** (220 mg, 0.48 mmol, 1 equiv) and **24** (60 mg, 0.136 mmol, 1 equiv). Purification by column chromatography (EA/PE) yielded the title compound **16** as a light yellow solid (67 mg, 0.085 mmol, 63% yield). m.p 151-153 °C. HPLC analysis: retention time = 3.933 min; peak area, 97.41%. ^{1}H NMR (300 MHz, Chloroform-*d*) δ 8.36 (s, 1H), 8.05 (s, 1H), 7.89 (s, 1H), 7.66 (dd, *J* = 7.8, 1.7 Hz, 2H), 7.54 – 7.41 (m, 3H), 7.14 – 7.02 (m, 3H), 6.92 (t, *J* = 7.6 Hz, 1H), 6.81 (d, *J* = 8.5 Hz, 1H), 6.59 (d, *J* = 7.5 Hz, 1H), 6.13 (s, 1H), 5.67 (s, 1H), 4.91 (d, *J* = 5.4 Hz, 1H), 4.12 (s, 3H), 3.31 (s, 3H), 3.20 -3.11 (m, 6H), 2.87 – 2.76 (m, 2H), 2.55 (t, *J* = 7.3 Hz, 2H), 1.53 (t, *J* = 7.3 Hz, 2H), 1.44 – 1.37 (m, 2H), 1.33 – 1.16 (m, 4H). HRMS-EI *m/z* [M+H] $^{+}$ calcd for $C_{40}H_{41}N_6O_9S^+$: 781.2650, found: 781.2648. ^{13}C NMR (101 MHz, Chloroform-*d*) δ 171.81 , 171.61 , 169.54 , 169.06 , 167.99 , 167.68 , 156.35 , 146.84 , 142.46 , 138.35 , 136.14 , 135.06 , 132.39 , 130.72 , 126.87 , 126.81 , 126.48 , 125.93 , 125.78 , 124.30 , 124.11 , 120.62 , 116.75 , 112.15 , 111.39 , 109.74 , 104.29 , 77.27 , 56.45 , 48.88 , 42.27 , 39.18 , 38.16 , 32.57 , 31.40 , 29.05 , 28.55 , 26.31 , 23.95 , 22.77 .

5.1.2.11

N-(6-((2-(2,6-dioxopiperidin-3-yl)-1,3-dioxoisoindolin-4-yl)amino)hexyl)-3-(6-((2-methoxyphenyl)sulfonamido)-1-methyl-2-oxo-1,2-dihydrobenzo[cd]indol-4-yl)propanamide (17). Compound **17** was prepared according to **13** in two steps, respectively, starting from **28c** (240 mg, 0.50 mmol, 1 equiv) and **24** (60 mg, 0.136 mmol, 1 equiv). Purification by column chromatography (EA/PE) yielded the title compound **17** as a light yellow solid (63 mg, 0.081 mmol, 59% yield). m.p 142-144 °C. HPLC analysis: retention time = 4.511 min; peak area, 96.29%.^{1}H NMR (300 MHz, Chloroform-*d*) δ 8.63 (s, 1H), 8.03 (s, 1H), 7.85 (s, 1H), 7.75 (s, 1H), 7.65 (d, *J* = 7.8 Hz, 1H), 7.47 (t, *J* = 8.0 Hz, 2H), 7.07 (dd, *J* = 10.9, 7.9 Hz, 3H), 6.90 (t, *J* = 7.7 Hz, 1H), 6.83 (d, *J* = 8.6 Hz, 1H), 6.59 (d, *J* = 7.6 Hz, 1H), 6.15 (s, 1H), 5.82 (d, *J* = 6.2 Hz, 1H), 4.94 (s, 1H), 4.11 (s, 3H), 3.30 (s, 3H), 3.17 (t, *J* = 7.7 Hz, 6H), 2.90 – 2.70 (m, 3H), 2.55 (t, *J* = 7.6 Hz, 2H), 2.20 – 2.09 (m, 1H), 1.48 (t, *J* = 7.2 Hz, 2H), 1.32 (dd, *J* = 19.2, 11.8 Hz, 4H), 1.15 (d, *J* = 7.5 Hz, 2H). HRMS-EI *m/z* [M+H] $^{+}$ calcd for $C_{41}H_{43}N_6O_9S^+$: 795.2807, found: 795.2797. ^{13}C NMR (101 MHz, Chloroform-*d*) δ 171.68 , 171.31 , 169.51 , 168.83 , 167.95 , 167.59 , 156.29 , 146.74 , 142.44 , 138.62 , 136.17 , 135.04 , 132.38 , 130.72 , 126.94 , 126.73 , 126.52 , 126.44 , 126.20 , 125.85 , 124.59 , 124.28 , 120.74 , 116.73 , 112.19 , 111.53 , 109.86 , 104.16 , 77.25 , 56.54 , 48.90 , 41.97 , 38.87 , 38.20 , 32.54 , 31.44 , 29.72 , 26.91 , 26.30 , 26.18 , 22.80 .

5.2. Protein Inhibition Assay

The differential scanning fluorimetry (DSF) was tested on a Mx3005p Real Time PCR machine (Stratagene) device. The NaCl, 10 nM HEPES, pH 7.5, and finally formulated into a 2 μM/20 μL solution in a 96-well plate. The compound **6** was added to the solution at a concentration of 10 μM while adding the fluorescent probe SYPRO Orange at a ratio of 1:1000. The excitation and emission wavelengths of SYPRO Orange are set at 465 nm and 590 nm, respectively. The temperature is raised from 25 °C to 96 °C by 3 °C per minute and fluorescence readings are taken at each interval. Then, according to the theoretical conversion formula between fluorescence intensity and temperature change, melting temperatures (Tm) were calculated by fitting the sigmoidal melt curve to the Boltzmann equation using GraphPad Prism. ΔTm is the difference in Tm values calculated for reactions with and without compounds. The larger the ΔTm value, the stronger the binding ability of the compound to the protein, on the contrary, the weaker the binding force.

The AlphaScreen assay (Amplified Luminescent Proximity Homogeneous Assay Screen) is used the binding assay of the readers, which was performed by *Reaction Biology Corp*. (Malvern PA) as described previously. The biotinylated peptide binding to the reader domain of His-tagged protein is monitored by the singlet oxygen transfer from the Streptavidin-coated donor beads to the AlphaScreen Ni-chelate acceptor beads. *Reaction Procedure:* 1. Deliver 2.5X BRD in wells of reaction plate except No BRD control wells. Add buffer instead. 2. Deliver compounds in 100% DMSO into the BRD mixture by Acoustic technology (Echo550; nanoliter range). Spin down and pre-incubation for 30 min. 3. Deliver 5X Ligand. Spin and shake. 4. Incubate for 30 min at room temperature with gentle shaking. IC_{50} values and curve fits were obtained by Prism (GraphPad Software).

5.3. The Cell Apoptosis Assay

The apoptosis of MV4-11 cells was determined by Annexin V-FITC/PI assay. Annexin V binds to phosphatidylserine, The externalization of phosphatidylserine is one of the leading indicators of apoptosis, which is one of the earliest indicators of cellular apoptosis located on the cell membrane. Propidium iodide (PI) is a popular red-fluorescent nuclear and chromosome counterstain. Since propidium iodide is not permeant to live cells, it is also commonly used to detect dead cells in apopulation. It can be used to differentiate necrotic, apoptotic and normal cells. Cells (2×10^5) were seeded in 6-well plate and were treated with varying concentrations of compounds for 24 h and 48 h. MV4-11 cells were collected and incubated with 5 μL of FITC-conjugated Annexin V (Nanjin keyGen Biotech Company). The nuclei were then counterstained with 5 μL of Propidium Iodide. After the dual staining, the cells were screened by a FAC Scan flow cytometer (FACS Calibun, Becton Dickinson). The upper left corner of the quadrant represents debris, lower left are live cells, upper right are advanced apoptotic or necrotic cells and lower right are apoptotic cells.

5.4. The Cell Cycle Assay

The Leukemia cells were treated with test compounds at different concentrations for 24 h. The prepared single cell suspension was fixed with a volume fraction of 70% ethanol for 2 hours (or overnight), stored at 4 °C and the fixative was washed away with PBS before staining (if necessary, the cell suspension was filtered once with a 200 mesh screen). Add 100 microliter RNase A 37 ° C water bath for 30 min; Add 400 microliter of PI stain and mix well, avoiding light for 30 min at 4 °C. On-machine detection, the red fluorescence was analyzed by flow cytometry using a 488 nm laser (Cell Lab Quanta SC, Beckman Coulter). Cell cycle analysis was made using a FACScan cytometer (FACSCalibun, Becton Dickinson).

5.5. The Cell Growth Inhibition Assay

media (Corning, USA) with 10% FBS and supplemented with 2% L-glutamine and 1% pen/strep. The MV4-11 cell line was maintained in culture media at 37 °C with 5% CO_2. The effects of target compounds on MV4-11 proliferation were performed by Nanjing Anacon Biotechnology Co., Ltd. Cells were cultured in 96-well culture plates (10000/well). The compounds of various concentrations were added into the plates. Cell proliferation was determined after treatment with compounds for 72 h. Cell viability was measured using the CellTiter-Glo assay (Promega, USA) according to the manufacturer's instructions, and luminescence was measured in a multilabel reader (Envision2014, PerkinElmer, USA). Data were normalized to control groups (DMSO) and represented by the mean of three independent measurements with standard error of <20%. IC_{50} values were calculated using Prism 5.0 (GraphPad Software, San Diego, CA).

5.6. The Western blotting

For Western blot analysis, 1.5 - 2 × 10^6 cells/well of MV4-11 cells were plated in 12-well plates and treated with compounds at the preset concentrations and times. Cells were collected, washed with cold PBS, and lysed in cold RIPA buffer containing Halt protease inhibitors. 20 μL lysate were run in each lane of 4−20% or 4−12% Novex gels and blotted into polyvinylidene difluoride membranes. The antibodies used for immunoblotting were BRD4 (BRD4 (E2A7X) Rabbit mAb #13440), c-Myc (Myc-Tag (71D10) Rabbit mAb #2278) and Santa Cruz Biotechnologies' GAPDH (GAPDH (D16H11) XP® Rabbit mAb #5174) purchased from Cell Signaling Technology.

5.7. Docking studies

3D structures of compounds **6** and **15** were built and minimized by the Ligand Preparation module in Schrodinger. Crystal structures of BRD4 (PDB ID: 3MXF) were downloaded from the Protein Data Bank (www.rcsb.org). After the non-essential waters were deleted and the hydrogen atoms were added to the protein, the protein was prepared using Protein Preparation Wizard in the Schrodinger suite. The Glide module with extra precision (XP) was selected for molecular docking. Compound **6** and **15** best conformations were minimized by a post docking program. Figures of docking result were presented by Pymol software (http://www.pymol.org).

Acknowledgments

We are grateful to the National Natural Science Foundation of China (Program No. 81673301) for financial support. This work was financially supported by the "Double First-Class" University project from China Pharmaceutical University (Program No. CPU2018GF02). A Project Funded by the Priority Academic Program Development of Jiangsu Higher Education Institutions (Integration of Chinese and Western Medicine), Jiangsu Province's Outstanding Leader Program of Traditional Chinese Medicine (SLJ0212). We also express our gratitude to the National Cancer Institute (Department of Health and Human Services, USA), Dr Ji Yu (KeyGen BioTech, Nanjing, China) and Dr Jamie Planck (RBC, Pennsylvania, USA) for their helpful support in biological evaluation.

References

1. P. Filippakopoulos, S. Picaud, M. Mangos, T. Keates, J.-P. Lambert, D. Barsyte-Lovejoy, I. Felletar, R. Volkmer, S. Müller, T. Pawson, Histone recognition and large-scale structural analysis of the human bromodomain family, *Cell*, 149 (2012) 214-231.
2. M.-M. Zhou, Structure and ligand of a histone acetyltransferase bromodomain, *Nature*, 399 (1999) 491.
3. H. Fukazawa, A. Masumi, The conserved 12-amino acid stretch in the inter-bromodomain region of BET family proteins functions as a nuclear localization signal, *Biol Pharm Bull.* (2012) b12-00527.
4. Q. Zhou, T. Li, D.H. Price, RNA polymerase II elongation control, *Annu Rev Biochem.* 81 (2012) 119-143.
5. P. Bandopadhayay, G. Bergthold, B. Nguyen, S. Schubert, S. Gholamin, Y.J. Tang, S. Bolin, S.E. Schumacher, R. Zeid, S. Masoud, F.R. Yu, N. Vue, W.J. Gibson, B.R. Paolella, S.S. Mitra, S.H. Cheshier, J. Qi, K.W. Liu, R. Wechsler-Reya, W.A. Weiss, F.J. Swartling, M.W. Kieran, J.E. Bradner, R. Beroukhim, Y.J. Cho, BET Bromodomain Inhibition of MYC-Amplified Medulloblastoma, *Clin Cancer Res.* 20 (2014) 912-925.
6. T. Takimoto-Shimomura, T. Tsukamoto, S. Maegawa, Y. Fujibayashi, Y. Matsumura-Kimoto, Y. Mizuno, Y. Chinen, Y. Shimura, S. Mizutani, S. Horiike, M. Taniwaki, T. Kobayashi, J. Kuroda, Dual targeting of bromodomain-containing 4 by AZD5153 and BCL2 by AZD4320 against B-cell lymphomas concomitantly overexpressing c-MYC and BCL2, *Invest. new drugs*, (2018).
7. K. Klein, P.A. Kabala, A.M. Grabiec, R.E. Gay, C. Kolling, L.L. Lin, S. Gay, P.P. Tak, R.K. Prinjha, C. Ospelt, K.A. Reedquist, The bromodomain protein inhibitor I-BET151 suppresses expression of inflammatory genes and matrix degrading enzymes in rheumatoid arthritis synovial fibroblasts, *Ann Rheum Dis.* 75 (2016) 422-429.
8. A. Nadeem, N.O. Al-Harbi, M.M. Al-Harbi, A.M. El-Sherbeeny, S.F. Ahmad, N. Siddiqui, M.A. Ansari, K.M.A. Zoheir, S.M. Attia, K.A. Al-Hosaini, S.D. Al-Sharary, Imiquimod-induced psoriasis-like skin inflammation is suppressed by BET bromodomain inhibitor in mice through RORC/IL-17A pathway modulation, *Pharmacol Res.* 99 (2015) 248-257.
9. C.J. Ott, N. Kopp, L. Bird, R.M. Paranal, J. Qi, T. Bowman, S.J. Rodig, A.L. Kung, J.E. Bradner, D.M. Weinstock, BET bromodomain inhibition targets both c-Myc and IL7R in high-risk acute lymphoblastic leukemia, *Blood*, 120 (2012) 2843-2852.
10. A.C. Belkina, G.V. Denis, BET domain co-regulators in obesity, inflammation and cancer, *Nat. Rev. Cancer*, 12 (2012) 465.
11. B. Padmanabhan, S. Mathur, R. Manjula, S. Tripathi, Bromodomain and extra-terminal (BET) family proteins: New therapeutic targets in major diseases, *J. Biosci.* 41 (2016) 295-311.
12. C.-W. Chung, Small molecule bromodomain inhibitors: extending the druggable genome, *Prog Med Chem.*, Elsevier2012, pp. 1-55.
13. P. Filippakopoulos, J. Qi, S. Picaud, Y. Shen, W.B. Smith, O. Fedorov, E.M. Morse, T. Keates, T.T. Hickman, I. Felletar, Selective inhibition of BET bromodomains, *Nature*, 468 (2010) 1067.
14. M.-M. Coudé, T. Braun, J. Berrou, M. Dupont, S. Bertrand, A. Masse, E. Raffoux, R. Itzykson, M. Delord, M.E. Riveiro, BET inhibitor OTX015 targets BRD2 and BRD4 and decreases c-MYC in acute leukemia cells, *Oncotarget*, 6 (2015) 17698.
15. E. Nicodeme, K.L. Jeffrey, U. Schaefer, S. Beinke, S. Dewell, C.-w. Chung, R. Chandwani, I. Marazzi, P. Wilson, H. Coste, Suppression of inflammation by a synthetic histone mimic, *Nature*, 468 (2010) 1119.
16. D. Chen, T. Lu, Z. Yan, W. Lu, F. Zhou, X. Lyu, B. Xu, H. Jiang, K. Chen, C. Luo, Discovery, structural insight, and bioactivities of BY27 as a selective inhibitor of the second bromodomains of BET proteins, *Eur. J. Med. Chem.*, 182 (2019) 111633.
17. S. Picaud, C. Wells, I. Felletar, D. Brotherton, S. Martin, P. Savitsky, B. Diez-Dacal, M. Philpott, C. Bountra, H. Lingard, RVX-208, an inhibitor of BET transcriptional regulators with selectivity for the second bromodomain, *Proc Natl Acad Sci.* 110 (2013) 19754-19759.
18. R.P. Law, S.J. Atkinson, P. Bamborough, C.-w. Chung, E.H. Demont, L.J. Gordon, M. Lindon, R.K. Prinjha, A.J. Watson, D.J. Hirst, Discovery of tetrahydroquinoxalines as bromodomain and extra-terminal domain (bet) inhibitors with selectivity for the second bromodomain, *J. Med. Chem.*, 61 (2018) 4317-4334.

highly BDII-selective BET family inhibitor ABBV-744 displays potent anti-tumor activity in androgen receptor positive prostate cancer models and an improved tolerability profile, *AACR*, 2018.
20. K.M. Sakamoto, K.B. Kim, A. Kumagai, F. Mercurio, C.M. Crews, R.J. Deshaies, Protacs: chimeric molecules that target proteins to the Skp1–Cullin–F box complex for ubiquitination and degradation, *Proc Natl Acad Sci*. 98 (2001) 8554-8559.
21. G.E. Winter, D.L. Buckley, J. Paulk, J.M. Roberts, A. Souza, S. Dhe-Paganon, J.E. Bradner, Phthalimide conjugation as a strategy for in vivo target protein degradation, *Science*, 348 (2015) 1376-1381.
22. K. Raina, J. Lu, Y. Qian, M. Altieri, D. Gordon, A.M.K. Rossi, J. Wang, X. Chen, H. Dong, K. Siu, PROTAC-induced BET protein degradation as a therapy for castration-resistant prostate cancer, *Proc Natl Acad Sci.* 113 (2016) 7124-7129.
23. C. Qin, Y. Hu, B. Zhou, E. Fernandez-Salas, C.-Y. Yang, L. Liu, D. McEachern, S. Przybranowski, M. Wang, J. Stuckey, Discovery of QCA570 as an exceptionally potent and efficacious proteolysis targeting chimera (PROTAC) degrader of the bromodomain and extra-terminal (BET) proteins capable of inducing complete and durable tumor regression, *J Med Chem.* 61 (2018) 6685-6704.
24. B. Zhou, J. Hu, F. Xu, Z. Chen, L. Bai, E. Fernandez-Salas, M. Lin, L. Liu, C.-Y. Yang, Y. Zhao, Discovery of a small-molecule degrader of bromodomain and extra-terminal (BET) proteins with picomolar cellular potencies and capable of achieving tumor regression, *J. Med. Chem.*, 61 (2017) 462-481
25. J. Hines, S. Lartigue, H. Dong, Y. Qian, C.M. Crews, MDM2-recruiting PROTAC offers superior, synergistic antiproliferative

of p53, *Cancer Res.*, 79 (2019) 251-262.
26. Y. Feng, S. Xiao, Y. Chen, H. Jiang, N. Liu, C. Luo, S. Chen, H. Chen, Design, synthesis and biological evaluation of benzo [*cd*] indol-2 (1*H*)-ones derivatives as BRD4 inhibitors, *Eur J Med Chem.* 152 (2018) 264-273.
27. X. Xue, Y. Zhang, Z. Liu, M. Song, Y. Xing, Q. Xiang, Z. Wang, Z. Tu, Y. Zhou, K. Ding, Discovery of Benzo [cd] indol-2 (1 H)-ones as Potent and Specific BET Bromodomain Inhibitors: Structure-Based Virtual Screening, Optimization, and Biological Evaluation, *J. Med. Chem.*, 59 (2016) 1565-1579.
28. E.S. Fischer, K. Böhm, J.R. Lydeard, H. Yang, M.B. Stadler, S. Cavadini, J. Nagel, F. Serluca, V. Acker, G.M. Lingaraju, Structure of the DDB1–CRBN E3 ubiquitin ligase in complex with thalidomide, *Nature*, 512 (2014) 49.
29. R.P. Nowak, S.L. DeAngelo, D. Buckley, Z. He, K.A. Donovan, J. An, N. Safaee, M.P. Jedrychowski, C.M. Ponthier, M. Ishoey, Plasticity in binding confers selectivity in ligand-induced protein degradation, *Nat. Chem Bio.* 14 (2018) 706.

Supplementary Material

The results of the compound **15** against NCI 60 cell lines, the IC_{50} curves of **15** against multiple cancer cell lines, the docking model of **15**, raw characterization data (including 1H NMR, 13C NMR spectra, HRMS spectrum and HLPC trace) for target compounds, the cell apoptosis assay and the cell cycle assay (.pdf)

Click here to remove instruction text...

Graphical Abstract

To create your abstract, type over the instructions in the template box below.
Fonts or abstract dimensions should not be changed or altered.

Discovery of Novel Small Molecule Induced Selective Degradation of the Bromodomain and Extra-Terminal (BET) Bromodomain Protein BRD4 and BRD2 with Cellular Potencies

Fei Jiang[a,b], Qingyun Wei [c,d], Huili Li[a], Hongmei Li[a], Yong Cui[a], Yu Ma[a], Haifang Chen[a], Peng Cao[c,d,*], Tao Lu[a,b,*], Yadong Chen[b,*].

[a] *School of Sciences, China Pharmaceutical University, 639 Longmian Avenue, Nanjing 211198, PR China.*
[b] *State Key Laboratory of Natural Medicines, China Pharmaceutical University, 24 Tongjiaxiang, Nanjing 210009, PR China.*
[c] *Affiliated Hospital of Integrated Traditional Chinese and Western Medicine, Nanjing University of Chinese Medicine, Nanjing 210028, PR China.*
[d] *Laboratory of Cellular and Molecular Biology, Jiangsu Province Academy of Traditional Chinese Medicine, Nanjing 210028, PR China.*

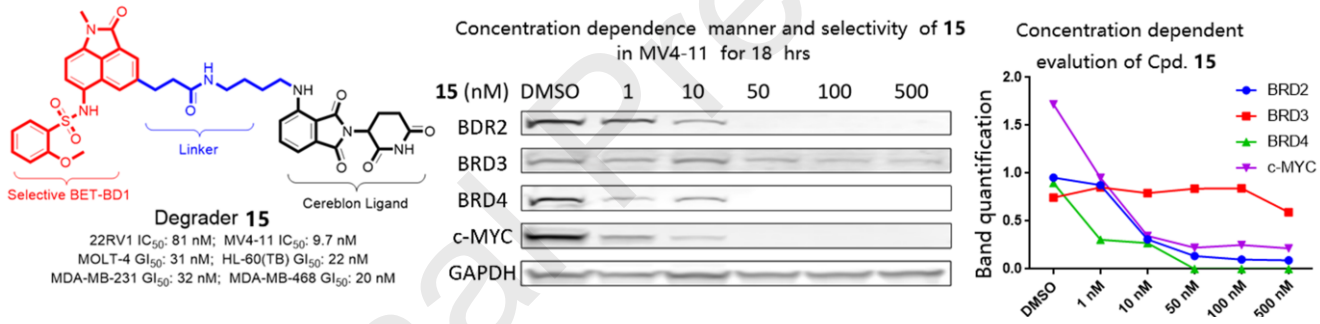

☒ The authors declare that they have no known competing financial interests or personal relationships that could have appeared to influence the work reported in this paper.

☐The authors declare the following financial interests/personal relationships which may be considered as potential competing interests: